Electronic Supplementary Material (ESI) for Physical Chemistry Chemical Physics.

Influence of counterions on the conformation of conjugated polyelectrolyte: the case of poly(thiophen-3-ylacetic acid)

Electronic Supplementary Information

Gregor Hostnik,[a] Matjaž Bončina,[a] Caterina Dolce,[b] Guillaume Mériguet,[b] Anne-Laure Rollet[b] and Janez Cerar[a]

1 Selected experimental details

1.1 Sample preparation

The chosen PTAA fraction was dissolved in 0.1 mol/dm^3 lithium hydroxide solution, filtered through the cellulose nitrate filter with pore size 1.2 μm (Sartorius, Göttingen, Germany). The sample was reprecipitated from solution using 0.1 mol/dm^3 HCl, the precipitate was isolated by centrifugation, and finally dissolved in a lithium hydroxide solution. When the polymer was fully dissolved, the solution was filtered through the cellulose nitrate filter with pore size 0.45 μm. Afterwards, HCl solution was added into filtrate in order to decrease the pH value of polymer solution to 5.1. This solution was dialysed in dialysis tubes (Spectra/Por 3, relative molecular mass cut-off 3.5 kg mol^{-1}) against triply distilled water for about one month. After dialysis the degree of neutralisation was increased to approximately 97 % using the appropriate hydroxide solution.

The PTALi stock solution, prepared as described in the previous paragraph, was frozen and light water (H_2O) was removed by freeze-drying. The dried sample was dissolved in a corresponding amount of heavy water (D_2O) to prepare a solution of the desired concentration. Before each experiment, concentration of the PTAA salt solution was checked at wavelength 311.0 nm.[1] Regarding NMR-experiments, low molecular mass salts (LiCl, NaCl, CsCl, tetramethylammonium chloride – TMACl, tetraethylammonium chloride – TEACl, tetrapropylammonium chloride – TPACl, and tetrabutylammonium chloride – TBACl) in dry form were dissolved in such amount of heavy water (D_2O) to obtain solutions with concentration of approximately 0.2 mol/dm^3. For UV/vis experiments low molecular mass salt solutions in H_2O with approximate concentration of 0.15 mol/dm^3 were prepared. In both cases exact concentrations of low molecular mass salt solutions were determined by potentiometric titrations with $AgNO_3$ as titrant at 298.15 K using a 736 GP Titrino (Metrohm, Switzerland) automatic titrator. In these titrations a chloride-selective electrode (Metrohm, Switzerland, type 6.0502.120) as an indicator electrode and a mercury(I) sulfate electrode as a reference electrode were used.

1.2 On the accuracy of self-diffusion coefficient measurement using PFG SE NMR

The accuracy of self-diffusion measurement by NMR is known to be about the 1-2 % when good conditions are met. In the present study, in certain cases poorer accuracy was obtained.

^{23}Na$^+$. In the case of ^{23}Na$^+$, the measurements are hindered by fast NMR relaxation rate of this quadrupolar nucleus. In fact, an important portion of the signal is lost during the diffusion time Δ in the NMR sequence, degrading considerably the signal-to-noise ratio. As explained detailed later on in the ESI subsection 3.3 about the relaxation rate of quadrupolar nuclei, the relaxation rate of quadrupolar ^{23}Na$^+$ nuclei are further increased when these nuclei experience close vicinity of the polyelectrolyte chain what leads to further deterioration of the signal-to-noise ratio. As a consequence, a large experimental error in solutions with low ^{23}Na$^+$ concentration (*i.e.* at low r_n values) is possible. In order to show possible error in determined f_{Na}, in Figure 2 (main text) results are represented by two points at each r_n value. One point (●) is estimated from the attenuation of peak intensity and the second one (○) from attenuation of peak area during increase of gradient strength. At high Na$^+$ concentrations, where signal-to-noise ratio is higher, both values are very close to each other.

TMA$^+$. The situation is different in the case of ^{1}H nuclei appurtenant to tetramethylammonium counterions. The relaxation rate of the ^{1}H is sufficiently low to keep most of the signal during the diffusion time in the NMR sequence. The difficulty comes from the overlap of the PTA$^-$ peak and the unique peak of TMA$^+$.

In Figure S1 example of ^{1}H NMR spectrum of mixture of PTALi with TBACl in D_2O ($c_p = 0.02$ monomol/dm^3, $r_n = 1.0$) is given in order to show the problem of peak overlap and how this problem is overcome in the case of tetraalkylammonium counterions with longer alkyl chains. In the case of mixture of PTALi and TBACl seven peaks may be observed in ^{1}H NMR-spectrum. Two low and broad peaks at approximately 3.00–3.75 ppm and 6.75–7.75 ppm correspond

[a] *Faculty of Chemistry and Chemical Technology, University of Ljubljana, Večna pot 113, SI–1000 Ljubljana, Slovenia. E-mail: janez.cerar@fkkt.uni-lj.si*
[b] *Sorbonne Universités, UPMC Univ Paris 06, CNRS, Laboratoire PHENIX, Paris, France*

to aliphatic and aromatic hydrogen atoms in PTAA, respectively. Four reasonably narrow and intensive peaks between approximately 3.00 and 0.75 ppm correspond to hydrogen atoms in TBA alkyl chains. The peak at 3.00 ppm belongs to hydrogen atoms being the closest to the quaternary nitrogen atom, and for remaining three groups of ^{1}H atoms in butyl chains the chemical shift diminishes with the increasing distance from the quaternary nitrogen atom. Peak at 4.8 ppm corresponds to traces of HOD in D_2O.

PTA$^-$. The principal reason for the uncertainty in the PTA$^-$ self-diffusion coefficients comes from the width of the polyion peaks in ^{1}H NMR-spectra what makes accurate integration difficult, as it can be seen in Figure S1.

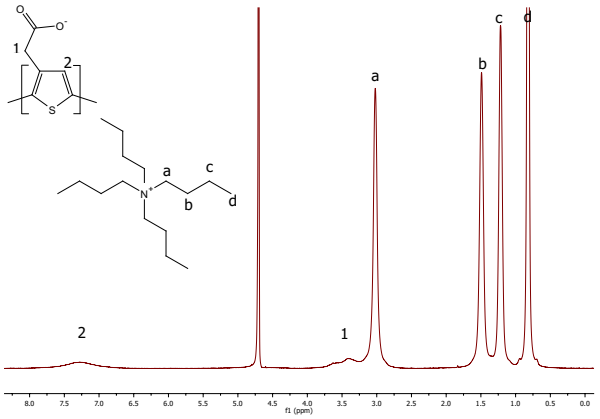

Fig. S1 ^{1}H NMR spectrum of PTALi and TBACl mixture at ratio $r_n = 1$.

>From Figure S1 one can see that peaks corresponding to TBA$^+$ ions are singlets instead of multiplets, what is a consequence of signal broadening due to interactions with PTA$^-$ polyion. Next observation is that the peak corresponding to hydrogen atoms nearest to quaternary nitrogen atom (denoted by 'a' in Figure S1) overlaps with the peak of PTA$^-$ aliphatic hydrogen atoms ('1'). Consequently, in order to avoid use of areas of these two peaks in determination of self-diffusion coefficients, the self-diffusion coefficient of polyion was determined from the peak corresponding to PTA$^-$ aromatic hydrogen atoms ('2'), while self-diffusion coefficient of tetraalkylammonium counterions was determined from the peaks corresponding to hydrogen atoms further away from quaternary nitrogen atom (in case of TBA$^+$ from peaks 'b'–'d'). This obstacle could not be overcome in the case of TMA$^+$ counterions taking that only one peak (at 3.0 ppm) belonging to ^{1}H atoms in TMA$^+$ exists. As a consequence TMA$^+$ self-diffusion coefficients are rather underestimated due to slow attenuation of the peak stemming from the aliphatic hydrogen atoms in PTA$^-$. The error is more pronounced at small values of r_n and becomes less important with increasing r_n.

2 Cylindrical cell model

In order to estimate the fraction of free counterions, f, in salt-free polyelectrolyte solution as well as in PE solution with simple salt added, Poisson-Boltzmann equation in cylindrical symmetry[2–4] was solved, and its solution used in theoretical prediction of f. This approach is based purely on electrostatic effects and ignores possible specific interactions stemming from hydrophobic effect.

In the frame of the applied theory, polyelectrolyte solution is depicted as an assembly of independent, identical, infinitely long and electroneutral cylindrical cells. Polyion with radius of a is placed on z-axis of each cell. The radius of the cell (R) is determined by the polyelectrolyte concentration c_p (expressed as molar concentration of repeating units)

$$c_p^{-1} = \pi R^2 N_A b, \tag{1}$$

where N_A represents Avogadro's number and b the distance between two successive charges on the polyion. To assure electroneutrality of the cell, the cell is filled with dimensionless counterions that counterbalance the charge of the polyion. In the case when simple salt is present in solution, additional co- and counterions have to be inserted in the cell. In cylindrical symmetry, Poisson-Boltzmann equation writes

$$\frac{1}{r}\frac{d}{dr}\left[r\frac{d\psi(r)}{dr}\right] = -\frac{\rho(r)}{\varepsilon_0\varepsilon_r} \tag{2}$$

where r denotes a distance from the cell axis, $\psi(r)$ represents electrostatic potential at radius r while ε_0 and ε_r stand for permittivity in the vacuum and relative permittivity of solvent, respectively. The local charge density, $\rho(r)$, at the distance r from the axis of the cell writes

$$\rho(r) = eN_A\sum_i c_i(R)\mathrm{e}^{-\frac{z_i e\psi(r)}{k_B T}} \tag{3}$$

where the index i indicates ionic species of type i, e elemental charge, $c_i(R)$ concentration of ionic species i at the outer border of the cell, k_B Boltzmann constant, and T temperature in K. In the case of a negatively charged polyion, the charge number is $z_i = +1$ for monovalent counterions and $z_i = -1$ for monovalent coions.

In order to solve equation 2, boundary conditions need to be known. The boundary condition at the outer border of the cell is given by expressions

$$\left(\frac{d\psi(r)}{dr}\right)_{r=R} = 0, \tag{4}$$

$$\psi(R) = 0, \tag{5}$$

while the one at the charged surface of the polyion follows from Gauss's law

$$\left(\frac{d\psi(r)}{dr}\right)_{r=a} = -\frac{2\xi}{a}. \tag{6}$$

The parameter ξ is called linear charge density and is common both to the cylindrical cell model approach and Manning's condensation theory. It is defined as the ratio of the Bjerrum length, l_B, to the charge separation distance b:

$$\xi = \frac{l_B}{b} = \frac{e^2}{4\pi\varepsilon_0\varepsilon_r k_B T b} \tag{7}$$

The differential equation 2 was solved numerically by the shooting method using the 4th order Runge-Kutta procedure.[5] Fractions of free counterions obtained[6] from self-diffusion coefficients were calculated[6–8] from the spatial dependence of the electrostatic potential ψ using equation 8 where angle brackets denote spatial average.

$$f = \frac{1}{\left\langle e^{-\frac{e\psi(r)}{k_b T}}\right\rangle \left\langle e^{\frac{e\psi(r)}{k_b T}}\right\rangle} \tag{8}$$

3 Fractions of free counterions determined by NMR

3.1 Dispersity effects

When using NMR diffusometry experiments on polymer solutions, particular expedients have to be considered. Polymer systems are polydisperse in nature and characterised by a range of molecular weights that give rise to a corresponding molecular size distribution and then a distribution of self-diffusion coefficients. Here the final expression used to analyse NMR data will be calculated in detail. First a general expression independent of the mass distribution will be found, and after then the log-normal distribution will be applied to obtain the final expression.

The ratio between measured intensity of NMR signal of the monodisperse polyion in the presence ($A(k)$) and in the absence (A_0) of magnetic field gradient, $A(k)/A_0$, is dependent on its self-diffusion coefficients D_p,[9]

$$\frac{A(k)}{A_0} = \mathrm{e}^{-kD_p} \tag{9}$$

where k ($= \gamma^2 g^2 \delta^2 (\Delta - \delta/3 - \tau/2)$) represents the diffusion sensitivity factor.[10] When polydisperse system is in question, a mass average dependence of ratio $A(k)/A_0$ has to be taken into account. Assuming that there are no interactions between coils of different molar mass (dilute system), one can adapt equation 9 to:

$$\frac{A(k)}{A_0} = \frac{\sum_i h_i M_i \exp(-kD_i)}{\sum_i h_i M_i} \tag{10}$$

where h_i is the number of polymer molecules of mass M_i and of diffusion coefficient D_i. For $|kD_i| < 1$ equation 10 may be expanded as a power series $\mathrm{e}^x = 1 + x + \frac{x^2}{2!} + \frac{x^3}{3!} + \ldots$ up to the second order in kD_i

$$\frac{A(k)}{A_0} = 1 - k\frac{\sum_i h_i M_i D_i}{\sum_i h_i M_i} + \frac{k^2}{2}\frac{\sum_i h_i M_i D_i^2}{\sum_i h_i M_i} \tag{11}$$

Further, equation 11 can be logarithmised and then expanded into series up to the second order, $\ln(1+x) = x - \frac{x^2}{2} + \cdots$, where $x = -k\frac{\sum_i h_i M_i D_i}{\sum_i h_i M_i} + \frac{k^2}{2}\frac{\sum_i h_i M_i D_i^2}{\sum_i h_i M_i}$. Upon disregarding terms of third and fourth order in D_i one obtains

$$\ln\frac{A(k)}{A_0} = -k\frac{\sum_i h_i M_i D_i}{\sum_i h_i M_i} + \frac{k^2}{2}\left[\frac{\sum_i h_i M_i D_i^2}{\sum_i h_i M_i} - \left(\frac{\sum_i h_i M_i D_i}{\sum_i h_i M_i}\right)^2\right] \tag{12}$$

which writes in terms of $\langle D\rangle_m$, the mass-averaged diffusion coefficient:

$$\ln\frac{A(k)}{A_0} = -k\langle D\rangle_m + \frac{k^2}{2}\left[\left\langle D^2\right\rangle_m - \langle D\rangle_m^2\right] \tag{13}$$

3.1.1 Log-normal distribution

A common distribution function used to describe the molar mass distribution is a log-normal distribution (in probability theory, a log-normal distribution is a continuous probability distribution of a variable whose logarithm is normally distributed):

$$P(x) = \frac{1}{x\sigma\sqrt{2\pi}}\exp\left(-\frac{(\ln(x) - \ln(x_0))^2}{2\sigma^2}\right) \tag{14}$$

where x is a general variable, x_0 is the median value and σ is a measure of the width of distribution. For any real number s, the s-th moment μ_s of the log-normal distribution writes :

$$\mu_s = e^{s\mu+\frac{1}{2}s^2\sigma^2} \tag{15}$$

where $\mu = \ln x_0$ and σ are the mean and standard deviation of the natural logarithm.

Rewriting M_n and M_w in an integral form we obtain:

$$M_n = \frac{\int MP(M)dM}{\int P(M)dM} = \frac{\mu_1}{\mu_0} = \mathrm{e}^{\mu+\frac{\sigma^2}{2}} \quad M_w = \frac{\int M^2P(M)dM}{\int MP(M)dM} = \frac{\mu_2}{\mu_1} = \mathrm{e}^{\mu+\frac{3}{2}\sigma^2} \tag{16}$$

Then, it comes

$$\mathrm{e}^{\sigma^2} = \frac{M_w}{M_n} = Đ_M \tag{17}$$

The following scaling law for the diffusion coefficient can be assumed:

$$D(M) = \beta M^{-\alpha} \tag{18}$$

where β is a proportionality constant and α is a system dependent positive parameter.

Using the integral definition of $\langle D\rangle_\mathrm{m}$ and $\langle D^2\rangle_\mathrm{m}$:

$$\langle D\rangle_\mathrm{m} = \frac{\int MP(M)D(M)dM}{\int MP(M)dM} = \beta\frac{\mu_{1-\alpha}}{\mu_1} = \beta\exp\left(-\alpha\mu + \frac{\sigma^2}{2}\left[-2\alpha+\alpha^2\right]\right)$$

$$\langle D^2\rangle_\mathrm{m} = \frac{\int MP(M)D^2(M)dM}{\int MP(M)dM} = \beta^2\frac{\mu_{1-2\alpha}}{\mu_1} = \beta^2\exp\left(-2\alpha\mu + \frac{\sigma^2}{2}\left[-4\alpha+4\alpha^2\right]\right)$$

the final expression that will be used to fit data using log-normal distribution is derived from eq. (13):

$$\frac{k^2}{2}\left[\langle D^2\rangle_\mathrm{m} - \langle D\rangle_\mathrm{m}^2\right] = \frac{k^2}{2}\langle D\rangle_\mathrm{m}^2\left[\frac{\langle D^2\rangle_\mathrm{m}}{\langle D\rangle_\mathrm{m}^2} - 1\right] \tag{19}$$

which, using

$$\frac{\langle D^2\rangle_\mathrm{m}}{\langle D\rangle_\mathrm{m}^2} = \mathrm{e}^{\sigma^2\alpha^2} = \left(\frac{M_w}{M_n}\right)^{\alpha^2}$$

gives

$$\ln\frac{A(k)}{A_0} = -k\langle D\rangle_\mathrm{m} + \frac{k^2}{2}\langle D\rangle_\mathrm{m}^2\left[\left(\frac{M_w}{M_n}\right)^{\alpha^2} - 1\right] \tag{20}$$

3.2 Fraction of free lithium counterions

Figure S2 is given to show the experimental error in determination of fraction of free lithium counterions (f_Li). We can see that despite notable scattering of experimental results among different series of experiments (*i.e.* additions of different salts), the data scattering is rather random (no clear trend related to the size or hydration enthalpy of added counterions can be found). Values of f_Li seems to be the lowest in the case of addition of LiCl to PTALi at almost all studied r_n ratios but these deviations are too small to be undoubtedly confirmed. For example, measurements for addition of LiCl to PTALi were done twice (both data are plotted in Figure S2) for r_n values of 0.75, 1, and 2.5. The gap between both values at the same r_n can serve as a hint of possible error in the estimation of f_Li. In the lack of reliable evidence it is assumed that the displacement of bound lithium counterions by the added counterions is of statisti-

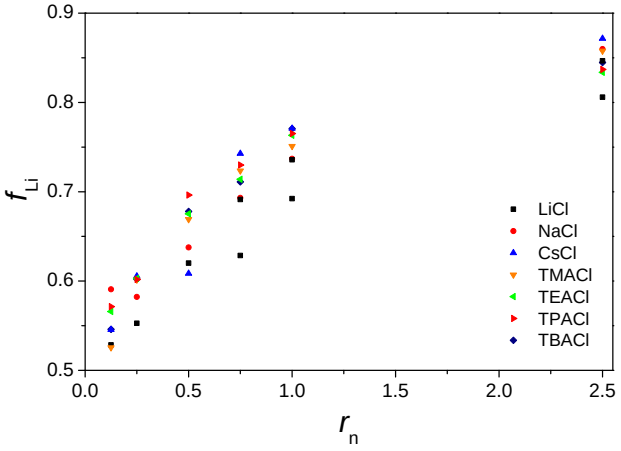

Fig. S2 Fraction of free Li^+ counterions (f_Li) as a function of the ratio r_n between concentration of added counterions and polyion's monomeric units. Results were obtained during mixing 0.02 monomol/dm^3 PTALi aqueous solution with various alkali metal and tetraalkylammonium chloride 0.2 mol/dm^3 solutions.

cal nature and that the observed differences are within the limits of experimental error.

Taking this into account, the fractions of f_{Li} at given r_n values are in Figure 2 in the main article represented as an average value of f_{Li} obtained from different series at the same r_n. The scattering of the data from different series at the same r_n is in Figure 2 (main article) represented by the error bars.

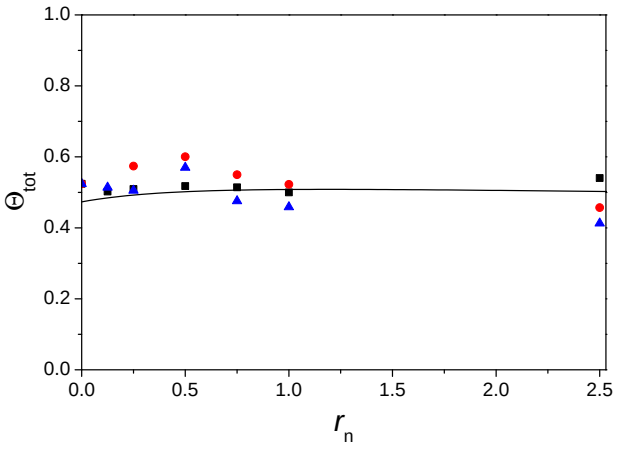

Fig. S3 Total fraction, θ_{total}, of occupied binding sites on PTA^- upon addition of alkali metal chlorides (LiCl – ■, NaCl – ●, and CsCl – ▲). Black line represents θ_{tot} calculated from the solution of Poisson-Boltzmann equation.

In Figure S3, the total fractions of occupied binding sites, θ_{tot}, on PTA^- upon addition of alkali metal chlorides are represented. Experimental values (symbols) are calculated as

$$\theta_{tot} = (1 - f_{Li}) + r_n \cdot (1 - f_{add}) \quad (21)$$

where f_{add} stands for fraction of free added counterions (Na^+ or Cs^+). In the case of addition of Li^+ equation simplifies to

$$\theta_{tot} = (1 - f_{Li}) \cdot (1 + r_n) \quad (22)$$

We can see that fraction of occupied binding sites on polyion is almost independent of the ratio r_n. The differences between θ_{tot} for additions of different salts are in the range of experimental error. The fractions of occupied binding sites θ_{tot} calculated from the solution of Poisson-Boltzmann equation in cylindrical symmetry are in rather good agreement with experimental values.

3.3 Relaxation of ^{7}Li and ^{133}Cs nuclei

An additional piece of information concerning counterion binding can be obtained from longitudinal relaxation times T_1 of counterions. In Figure S4, T_1 of $^7Li^+$ and $^{133}Cs^+$ are plotted as a function of r_n. Both types of nuclei have spin larger than $\frac{1}{2}$ ($\frac{3}{2}$ in the case of $^7Li^+$ and $\frac{7}{2}$ in the case of $^{133}Cs^+$) thus quadrupolar mechanism plays an important role in the returning of magnetisation towards equilibrium. Quadrupolar relaxation is a consequence of interaction of nuclei with spin $> \frac{1}{2}$ with electrical field gradient and it is accelerated by larger fluctuations in electric field gradient.

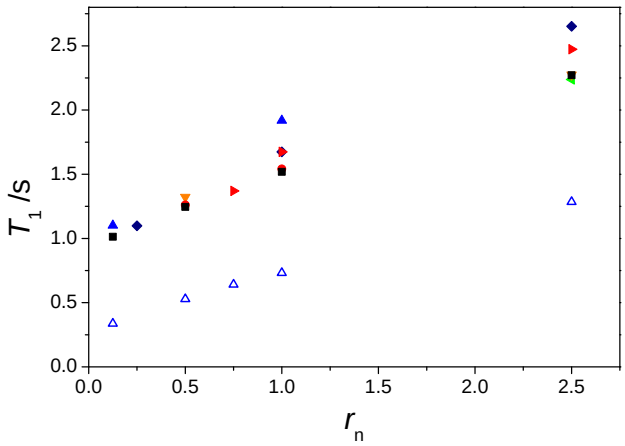

Fig. S4 Longitudinal relaxation time (T_1) of $^7Li^+$ and $^{133}Cs^+$ counterions as a function of r_n for titration with LiCl (■), NaCl (●), CsCl (▲, △), TMACl (▼), TEACl (◀), TPACl (▶), and TBACl (◆). Solid symbols represent T_1 of $^7Li^+$ while empty symbols represent T_1 of $^{133}Cs^+$ counterions.

In the present case, $^7Li^+$ and $^{133}Cs^+$ counterions experience larger fluctuations of electric field gradient (i) when they are in the immediate vicinity of the polyion (fluctuations are here more pronounced than at larger distances from the polyion) and (ii) when dehydration of these counterions takes place (dehydration substantially changes electric field in the local environment of the counterion[11]). Both these conditions are far more likely to be met when counterions are bound to the polyion than when counterions are "free". Since f increases when r_n increases, T_1 should increase with r_n. Indeed, the observed increase in T_1 values (see Figure S4) with increasing simple salt concentration is in good agreement with results of previous studies[12] and with fractions of free counterions obtained in the present paper (see Figures 2 and 3 of the main article).

References

1 G. Hostnik, V. Vlachy, D. Bondarev, J. Vohlídal and J. Cerar, *Acta Chim. Slov.*, 2012, **59**, 571–581.

2 A. Katchalsky, *Pure Appl. Chem.*, 1971, **26**, 327–374.

3 D. Dolar, in *Polyelectrolytes*, ed. E. Sélégny, M. Mandel and U. P. Strauss, D. Reidel, Dordrecht, Netherlands, 1st edn, 1974, vol. 1, pp. 97–113.

4 J. Piñero, L. B. Bhuiyan, J. Reščič and V. Vlachy, *Acta Chim. Slov.*, 2008, **55**, 521–527.

5 W. H. Press, B. P. Flannery, S. A. Teukolsky and W. T. Vetterling, *Numerical recipes in C++*, Cambridge University Pres: Oxford, 1992, pp. 650–694.

6 S. Lifson and J. L. Jackson, *J. Chem. Phys.*, 1962, **36**, 2410–2414.

7 J. R. Huizenga, P. F. Grieger and F. T. Wall, *J. Am. Chem. Soc.*, 1950, **72**, 2636–2642.

8 J. L. Jackson and S. R. Coriell, *J. Chem. Phys.*, 1963, **38**, 959–968.

9 P. T. Callaghan and D. N. Pinder, *Macromolecules*, 1983, **16**, 968–973.

10 D. Wu, A. Chen and C. Johnson, *J. Magn. Reson. A*, 1995, **115**, 260–264.

11 K. G. Victor, C.-L. Teng, T. R. D. Dinesen, J.-P. Korb and R. G. Bryant, *Magn. Reson. Chem.*, 2004, **42**, 518–523.

12 C. J. M. Van Rijn, A. J. Maat, J. De Bleijser and J. C. Leyte, *J. Phys. Chem.*, 1989, **93**, 5284–5291.